

# RAPID TERRAIN ANALYSIS IN LANDSLIDE ZONES: GPR AND AIRBORNE PHOTOGRAMMETRY AS A COMPLEMENT FOR THE LEVELLING DATA. CASE STUDY NEAR POIANA RUSCĂ DAM, ROMANIA

ALEXANDRA G. GERE<sup>1,2,3</sup>, ANDREI E. MIHAI<sup>1</sup>

<sup>1</sup>National Institute for Earth Physics Romania (INCDFP), 12 Călugăreni St., 077125, Măgurele, Ilfov, România

<sup>2</sup>University of Bucharest, Doctoral School of Geology, 1 Nicolae Bălcescu Blvd., 01004, Bucharest, Romania

<sup>3</sup>University of Birmingham, School of Engineering, Y8, Edgbaston, Birmingham, B15 2FG, United Kingdom  
e-mail: science.alexandra@gmail.com

**Abstract.** This paper investigates rapid terrain analysis in landslide-prone areas, emphasising a case study near the Poiana Ruscă Dam, Romania. The research integrates Ground Penetrating Radar (GPR) and airborne photogrammetry, complemented by traditional levelling data, to assess a known landslide with small dimensions on the southwest side of the Poiana Ruscă Lake, near the dam's upstream side. This landslide is part of an annual topo-geodetical monitoring campaign due to its potential impact on the dam's stability. The study utilises a compact drone to generate orthophotomosaics and Digital Elevation Models (DEMs) for the road sections above the landslide, identified in topo-geodetical records. This method offers high-resolution surface deformation data, providing a clear view of the impact on the affected road. The GPR method, employing a 200 MHz antenna, plays a crucial role in revealing subsurface details, particularly in areas where traditional levelling surveys face challenges due to disappearing benchmarks caused by terrain movement. This method effectively highlights areas of interest in the form of potential subsidence areas and voids, correlating with surface observations. Notably, the GPR data indicates stronger signal attenuation at relatively shallow depths, suggesting alterations in the subsurface composition and moisture content. These findings are critical for understanding the landslide's structural characteristics and its ongoing dynamics. This research demonstrates the synergy of GPR, airborne photogrammetry, and levelling data in providing a comprehensive analysis of landslide zones at a relatively fast and efficient pace. It emphasises the importance of integrating various technological approaches for effective monitoring and management of such geohazards, particularly in the context of maintaining the safety and integrity of hydropower dams and their surrounding infrastructure.

**Key words:** UAV, photogrammetry, GPR, Ground Penetrating Radar, topo-geodetical, levelling method, landslides, drone

## 1. INTRODUCTION

This paper presents an in-depth analysis of rapid terrain assessment in landslide zones, more specifically near the Poiana Ruscă dam in Romania. The study focuses on the integration of Ground Penetrating Radar (GPR) and airborne photogrammetry, complementing traditional levelling data, to enhance our understanding of the landslide dynamics in this area.

The Poiana Ruscă dam, a key infrastructure in the region, necessitates continuous monitoring due to its vulnerability

to landslides. In the vicinity of the dam, specifically on the southwest side of Poiana Ruscă Lake near the upstream area, lies a known landslide of small dimensions (Hidroconstrucția). This landslide is part of the annual topo-geodetical monitoring campaign for the dam, given its potential impact on the dam's stability and safety.

Slope stability in valleys where dams are constructed is a critical factor in the design and maintenance of these structures. The integrity of a dam is inextricably linked to the stability of its surrounding slopes, as any movement or failure

can have catastrophic consequences. Slopes in valley regions are often subject to various natural and anthropogenic factors that can compromise their stability, such as seismic activity, hydrological changes, and the construction process itself. Landslide occurrence in these regions is not just a risk during the construction phase but remains a continual threat throughout the lifespan of a dam. The fluctuating water levels in the reservoir can lead to the saturation of adjacent slopes, weakening soil and rock strength and increasing the likelihood of landslides.

In our study, a compact drone was employed to create orthophotomosaics and Digital Elevation Models (DEMs) for sections of the road above the landslide zone, as identified in the topo-geodetical records. These methods offer a rapid and detailed perspective of the terrain (Knyaz and Chibunichev, 2016), complementing the standard practices (Altaweel *et al.*, 2022). The choice of GPR for this investigation was motivated by its ability to provide rapid, in-depth insights into the subsurface structures beneath the road (Bianchini *et al.*, 2019) and the landslide (Borecka *et al.*, 2015; Ullah *et al.*, 2022). This method is crucial for understanding the internal characteristics of the landslide, which are essential for assessing its current state and predicting future behaviour. Additionally, this paper discusses the integration of traditional levelling data (Păunescu *et al.*, 2010), a standard norm in Romania for monitoring displacements and deformations in hydropower dams. The combination of these advanced methods with conventional techniques aims to provide a more comprehensive understanding of the landslide's dynamics, contributing valuable information for the ongoing monitoring and maintenance of the Poiana Ruscă Dam.

Through this case study, we aim to demonstrate the efficacy of combining GPR, airborne photogrammetry, and levelling data in rapidly assessing and monitoring landslide-prone areas, particularly in the context of dam safety and environmental management.

## 2. MATERIALS AND METHODS

In recent years, advanced technologies such as UAV-based surveys (Sun *et al.*, 2024), and geophysical methods like GPR have become invaluable tools for monitoring slope stability and landslides (Borecka *et al.*, 2015; Ullah *et al.*, 2022) in these sensitive areas. These methods allow for highlighting deformations both at the surface and subsurface, and potential instability, enabling timely preventative measures. The integration of such technologies with traditional topo-geodetical investigations forms a robust approach to ensuring the safety and longevity of dam infrastructures and the communities they serve.

### 2.1. LOCATION AND SITE DESCRIPTION

Situated on the southern flank of the Țarcu Mountains, approximately 8 km upstream from the Rusca commune, the Poiana Ruscă development is advantageously located

in a natural depression within a narrower region of the Rîul Rece. The area is characterised by relatively high-quality rock formations. The catchment area of the river basin in this segment encompasses 142 km<sup>2</sup>, with the Rîul Rece exhibiting an average discharge of 4.40 m<sup>3</sup>/s (Hidroconstrucția).

Initially the project of the dam was conceived differently, proposing the construction of a 95-metre-high arched concrete dam, capable of creating a reservoir with a volume of 50.9 million cubic metres and the work even commenced based on these parameters. However, post-1989, due to constrained financial resources, the project underwent a less ambitious redesign. This resulted in the construction of a dam with a reduced height of 75 m and a corresponding reservoir capacity of 35 million cubic metres. This modification is reflected in the dam's cross-sectional design, which features a foundational block up to the elevation of 575 m above mean sea level (as per the original design), surmounted by the arched structure as realised in the final version (Hidroconstrucția). Therefore the works started in 1987, stopped after 1990, resumed after 2002 and it was commissioned in 2009.

The slopes surrounding the entire basin generally exhibit robust stability, with the exception of a segment approximately 500 metres in length situated on the left bank (Fig. 1), extending immediately upstream of the dam, which represents the area upon which this project is focused. In terms of geological features, the composition at the dam site and area is diverse, and it includes quartzite, shale, chlorite phyllite, conglomerate, sandstone, and clay shale, underlain by a layer of covering deposits measuring 6-8 m in thickness (Hidroconstrucția).

### 2.2. LEVELLING METHOD

The topo-geodetic method used in this study represents the geometric levelling method, a method which is typically used in monitoring building subsidence involving levelling marks (bench marks) placed in the structure (Coșarcă, 2003). Aligning the levelling marks with fixed external reference points form the levelling network. This can vary in structure, often comprising closed polygons or parallel traverses, depending on the object's size and shape. It includes marks on the observed structure and external control marks, with their design influenced by local conditions and the construction's material (Fig. 2).

At the left slope of the Poiana Ruscă dam, the levelling network which monitors the landslide is formed of 4 fundamental (fixed) marks, and 11 levelling benchmarks, placed on both sides of the DJ608 road (Fig. 2). Another set of 16 levelling benchmarks are placed further east on the side of the DJ608 road facing the lake. Through the years, due to active type of landslide occurring on the monitored area, some of the marks have already suffered movement and damage in some instances themselves, which made some these marks for surveying, therefore reducing the

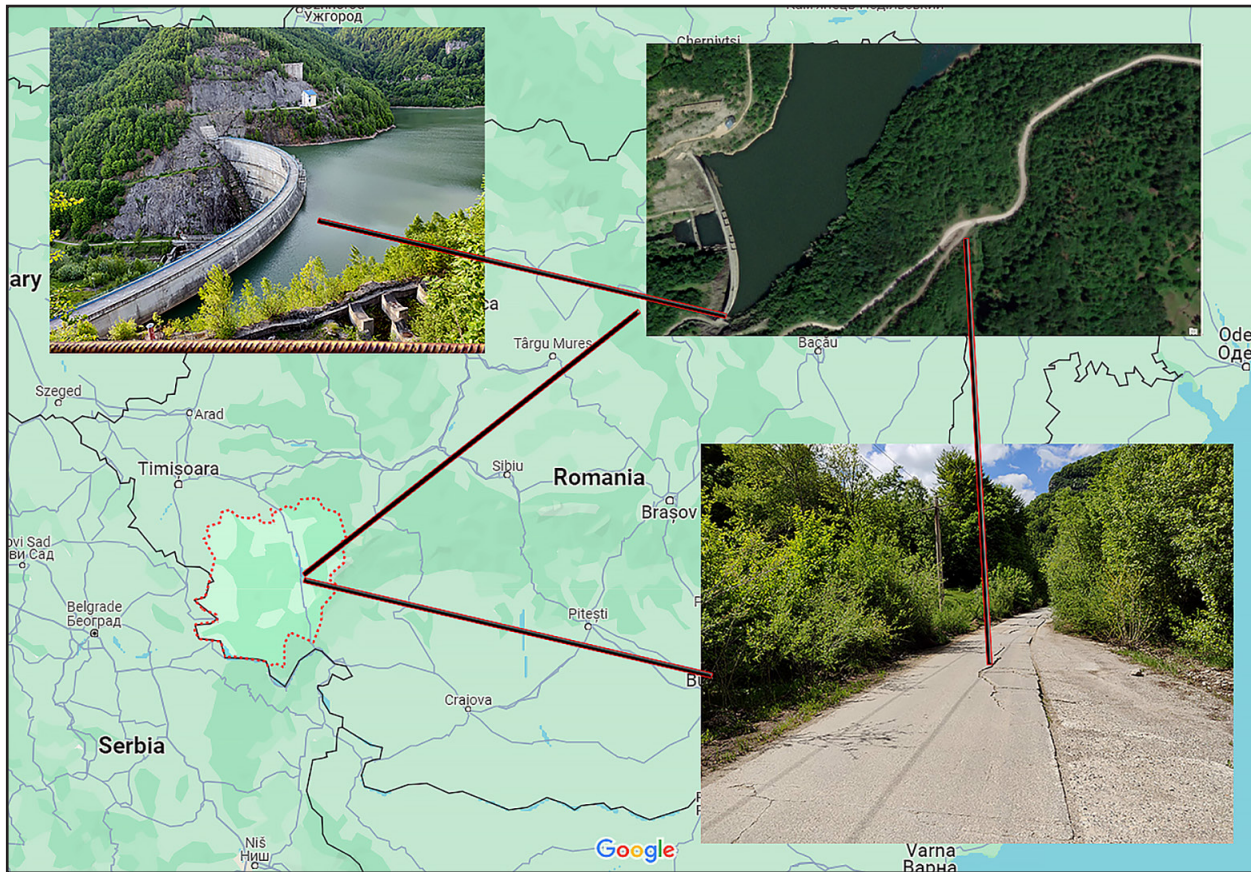


Fig. 1. Location of the survey area, near the Poiana Ruscă dam in the Caraș Severin county, Romania.

consistency in number of readings occurring every year, and lowering the amount of information to be correlated in some specific areas.

For the levelling data acquisition, the Leica digital level 250M was used along with a 3 m fiberglass barcode staff, achieving a precision of  $\pm 0.7$  mm per double kilometre of levelling. Geometric levelling with dual horizons was selected to ascertain vertical displacements. Additionally, to counteract staff sole degradation errors, each traverse began and ended with the same staff, and the spans were kept under 25 metres.

The levelling network was compensated using the method of conditional measurements of different precision, where the conditions refer to the unclosed readings polygon where the sum of all of the readings in the polygon should be 0 (Păunescu *et al.*, 2010), and the number of equations is given by the number of conditions. For each polygon considered the unclosed polygon was determined with its value found in the unclosed vector  $w$ . The coefficients of the conditional equations are represented inside the  $A$  matrix, and the weight matrix  $P$  created based on the distances between the position of the benchmarks (Păunescu *et al.*, 2010). Using these two matrices,  $A$  and  $P$  the normal system matrix  $N$  is calculated using formula (1), which is later used for creating the correlation vectors  $k$  based on the formula (2).

$$N = A^T P^{-1} A \quad (1)$$

$$k = N^{-1} w \quad (2)$$

The corrections are therefore applied to the measured level differences with the correction vector  $v$  calculated with formula (3). The empirical standard deviation of the weight unit is given by (4), where  $r$  represents the number of equations used (Păunescu *et al.*, 2010).

$$v = P^{-1} k A^T \quad (3)$$

$$S_0 = \sqrt{\frac{P v v^T}{r}} \quad (4)$$

### 2.3. AIRBORNE PHOTOGRAMMETRY

The areas chosen for the airborne surveys (Fig. 3) was as follows: one corresponding to the landslide area marked in the levelling network plan, where the road was visibly damaged at the surface; the second one is outside the levelling network on the same DJ608 road more to the east, in an area also clearly affected by land movements visible in the abundant cracks in the road.

For this study, the DJI Mavic Mini 2 drone has been used with a weight of 249 g, equipped with a 12 MP camera featuring image stabilisation and a gimbal with a mechanical range spanning from  $-110^\circ$  to  $35^\circ$ , rendering it apt for photogrammetric applications.



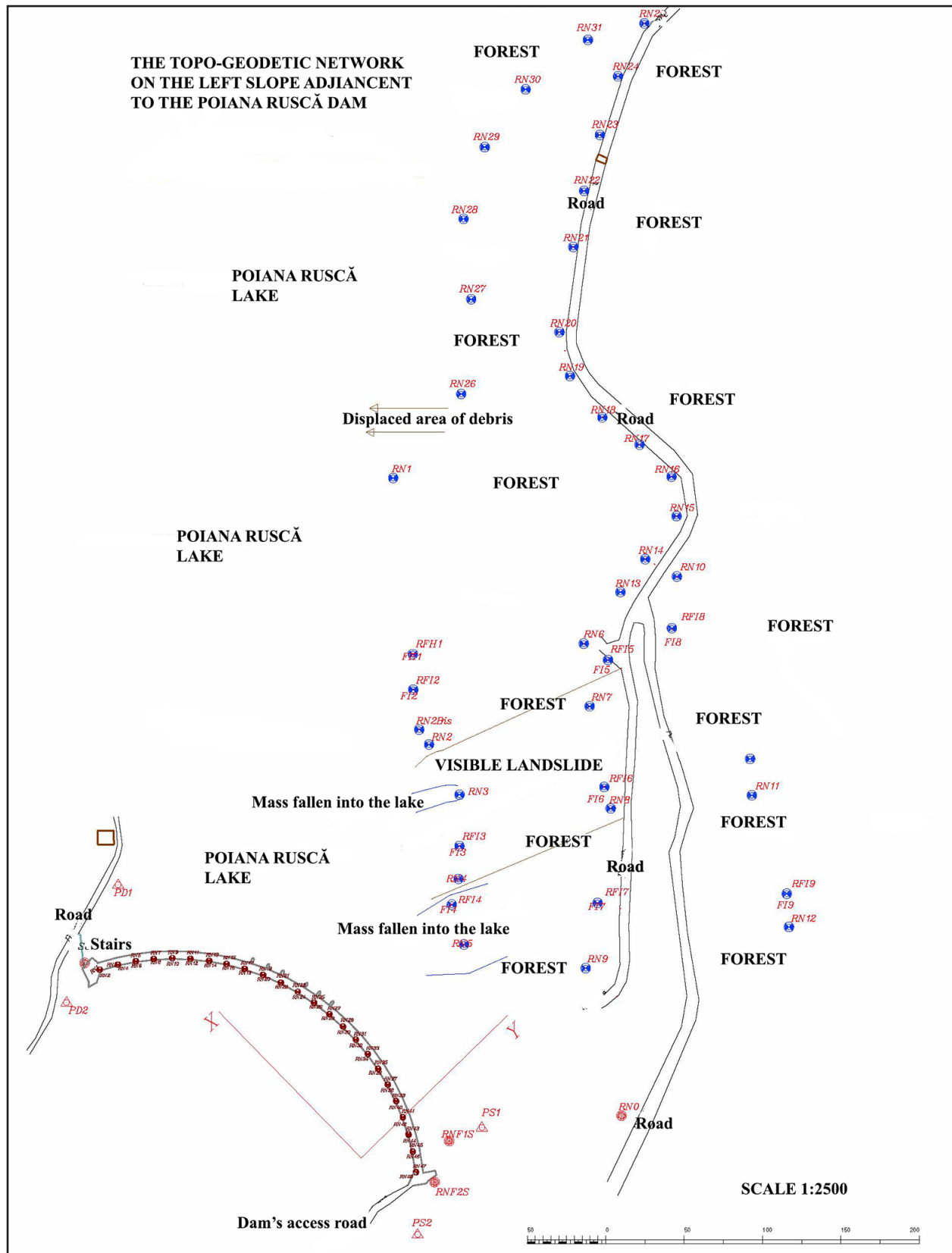


Fig. 2. The topo-geodetic network plan of the area of interest characterised by landslides, adjacent to the Poiana Ruscă dam.



**Fig. 3.** Overview from ArcGIS representing the overlapping of the topo-geodetic network plan with the airborne photogrammetry surveys.

Even though the drone is not specialised for these kinds of studies it has garnered recognition in academic literature for its diverse applications (Stankovic *et al.*, 2021) and it appears that it surpasses expectations for a diverse field of studies. The UAV incorporates standard GPS+GLONASS+GALILEO positioning systems, and benefits from a Visual Positioning System (VPS) which augments its positioning accuracy and can enhance vertical hovering accuracy from 0.5 m (GPS) to 0.1 m, and horizontal accuracy from 1.5 m (GPS) to 0.3 m (VPS).

For data acquisition the Drone Harmony software was used as it appears to have more comprehensive survey acquisition capabilities and allows for more flexibility in terms of planning the surveys, by allowing the user to specify flight parameters such as altitude, photo interval, and camera angle. Initially, flight plans were automatically set with camera angles of 90° and 60° at a 12 m altitude, as it appears to be a good altitude to provide enough coverage and information about the elevation for evaluating road surface deformations (Mugnai *et al.*, 2022). In densely vegetated areas, manual flight was employed to compensate. The automated flights maintained a 60% image overlap; a similar overlap was aimed for during manual flights, although the flight altitude varied under manual control. The outcome of this process was a collection of georeferenced images with partial overlap, which were imported into AgiSoft Metashape for standard processing. The initial step in the data processing involves selecting overlapping pixels to generate a point

cloud. Subsequently, leveraging the estimated camera positions and angles, a more comprehensive point cloud is constructed. For ensuring accuracy in terms of positioning, several ground control points have been used (road markers or distinct vegetation). This enhanced point cloud facilitates the creation of a triangular mesh, an orthomosaic, and a digital elevation model (DEM).

#### 2.4. GROUND PENETRATING RADAR

Ground Penetrating Radar (GPR) represents a non-invasive geophysical technique, which uses electromagnetic waves for subsurface imaging with applications, ranging from archaeology to geotechnics and geological studies (Reynolds, 2011). Its geotechnical applications include monitoring infrastructure like roads, bridges, and dams, crucial for their safety and longevity due to potential degradation over time (Rasol *et al.*, 2022).

GPR equipment typically consists of a control console, a distance-measuring wheel, and an antenna (Daniels, 2004) with the role of transmitting electromagnetic pulses, which, upon encountering materials with varying permittivity, reflect signals back. These returning signals form the so-called radargram, a two-dimensional image displaying subsurface anomalies (Conyers, 2004). The data, initially in the time domain, undergoes migration for spatial representation (Reynolds, 2011). Antenna frequency selection is critical, balancing between detail and penetration depth, normally higher frequencies provide better resolution but lower depth penetration, whereas



low frequencies manage to provide more information from deeper layers but with a loss in resolution (Daniels, 2004). In geotechnical studies and the assessment of road stabilities, GPR's utility lies in its ability to characterise internal structures and identify features like voids or subsidence (Buseti *et al.*, 2020) and fractures in roads and concrete (Rhazi *et al.*, 2004). The GPR method is increasingly recognized as a critical tool in landslide assessment and management. Its ability to provide subsurface images is essential for understanding the internal structure of landslides and the underlying geological conditions (Borecka *et al.*, 2015). In landslides, GPR is used to identify key features like the depth of the slip surface, the thickness of the landslide mass, and the presence of water or voids within the landslide body. This information is crucial for assessing landslide stability, potential reactivation, and for designing effective mitigation strategies. The high-resolution data obtained from GPR allows for a detailed characterization of the landslide, facilitating more accurate risk assessments (Sestras *et al.*, 2022). Roads impacted by landslides pose significant safety risks. GPR is used to assess the extent of subsurface damage and to identify areas where the road structure has been compromised. This includes detecting voids (De Giorgi *et al.*, 2014), cracks (Batrakov *et al.*, 2017), and weakened zones beneath the pavement that are not visible on the surface. Such assessments are crucial for road

repair and maintenance, ensuring that remedial actions are targeted and effective. One of the main advantages of GPR in these contexts is its non-invasive nature, allowing for rapid data collection without the need for extensive ground disturbance. This is particularly beneficial in areas where landslides have already caused instability, and where more invasive surveys like seismics in this case, would probably cause more problems. Furthermore, repeated GPR surveys can monitor changes over time, providing valuable data for ongoing landslide management and road maintenance.

At the surveys from the left slope adjacent to the Poiana Ruscă dam, a GSSI SIR-3000 with a 200 MHz (Fig. 4) antenna was employed. Despite the equipment's versatility, careful parameter selection is key for effective data acquisition. This antenna frequency was chosen with the purpose of collecting data from deeper layers and to manage to characterise the subsurface structure and find potential causes of the deformations and deteriorations on the road on which the surveys were carried out. A number of 10 profiles at a distance of 0.5m in between were carried out in the direction of the road, with profiles starting from the upper side of the slope and moving towards the lower side of the slope (towards the lake).



**Fig. 4.** The GPR equipment, formed of one 200 MHz antenna, a wheel for measuring distances and the GSSI-SIR 3000 console.

Only one set of data has been carried out, to assess its suitability on this type of setting, which also paves the way for more future surveys which would provide more information in terms of underground deformations over time.

The data was processed using ReflexW, a very popular GPR and seismic processing software in both academia and industry, and all radargrams followed the same steps and the same filter parameters which allows for better correlations of information throughout the profiles. The processing sequence starts with the geometrical corrections, after which 1D, 2D functions are used to remove unwanted noise, in the end the data being amplified to gain more visibility for the objectives of interest and migrated for transforming from the time domain into distances. A variety of processing steps and filters have been tested and analysed, until the following sequence has been found to highlight features of interest without overly distorting the underlying information. The specific data processing functions and their order is as follows:

- (i) For adjusting the zero time, the 'move starttime' function has been used.
- (ii) Low-frequency noise was mitigated using the 'subtract-mean' (dewow) function.
- (iii) Frequencies outside the antenna's operational range were removed with the 'butterworth bandpass filter,' targeting both low and high-frequency ranges.
- (iv) Systematic coherent noise was reduced by applying the 'background removal' function.

(v) Signal amplification was conducted using the energy decay gain function.

(vi) Even though migration was not applied, the hyperbola adjusting tool has been used to calculate a mean velocity of the environment (found to be at around 0.055 - 0.65)

After data processing, several elements could be identified and delimited in vertical profiles across the whole data set.

### 3. RESULTS AND DISCUSSION

All of the data has been added into a GIS project in ArcGIS Pro for a better visualisation and analysis of the data.

In terms of levelling data and information these are represented in terms of elevation differences compared to preset 0 elevation (Figs. 5-6). The data has been split in two graphs for better visualisation and to mark two areas - the one on the west side - closer to the dam and affected by the visible landslide, and the second one to the east, furthest away from the dam along the road. The marks which suffered damage or couldn't be found in the field were removed altogether from the graphs. For example RN3 benchmark (Fig. 2) due to its position in the fallen mass in the lake in the area of the visible landslide, this was not found and data is not available for it since 2012. Other benchmarks which suffered similar problems are the combination of benchmarks and fixed marks, RN5, RF14 and F14 which are placed in the large mass fallen into the lake area, closer to the dam.

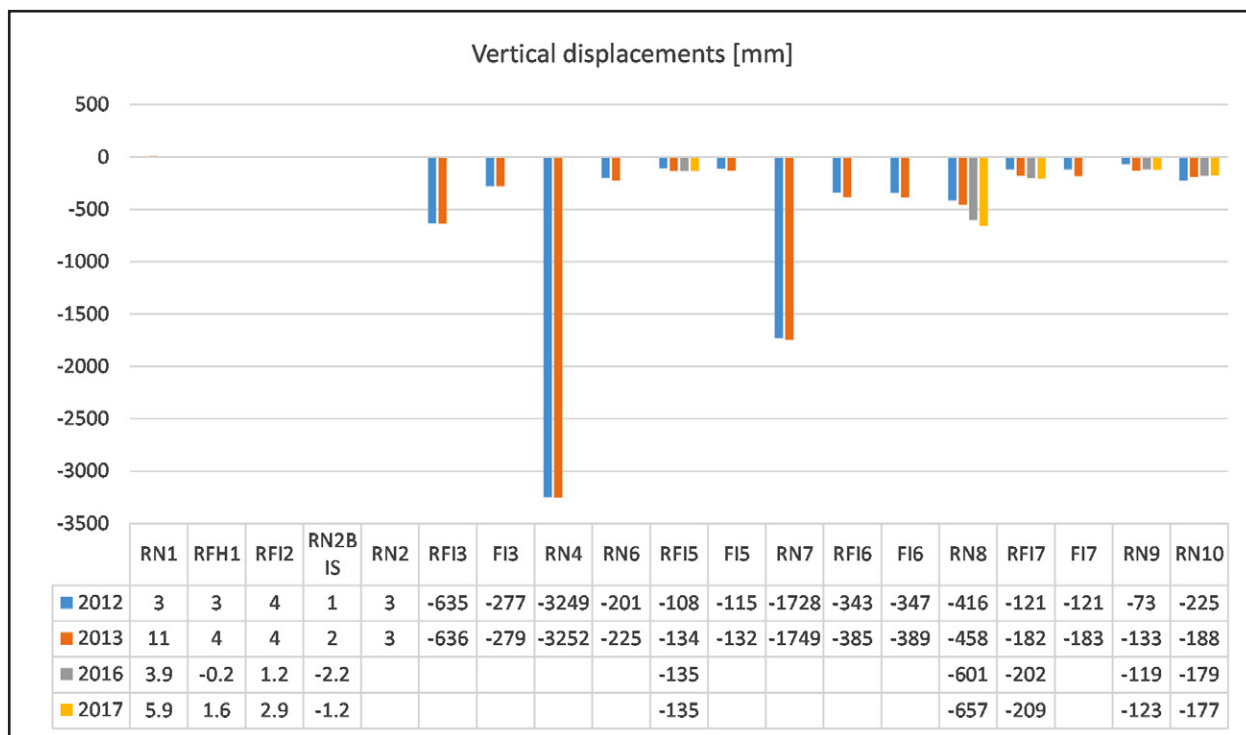


**Fig. 5.** Vertical displacements at the first half of the marks resulted from the levelling surveys. Missing data corresponds to the missing of the actual marks in the field throughout the years.



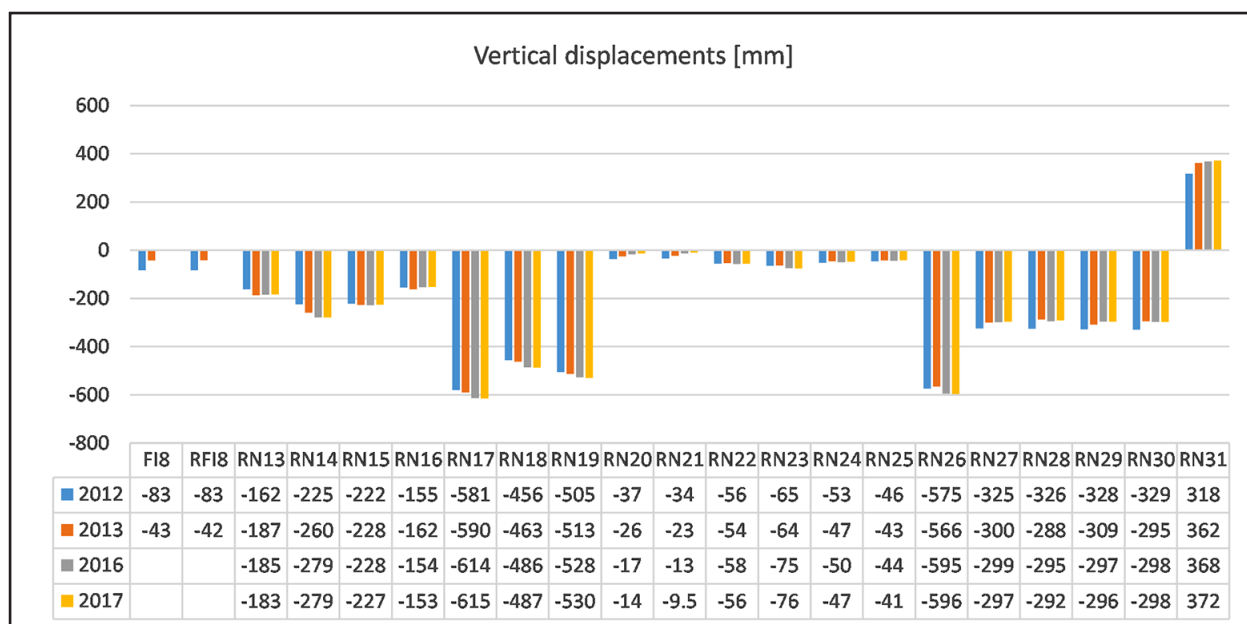


**Fig. 6.** Vertical displacements at the second half of the marks resulted from the levelling surveys. Missing data corresponds to the missing of the actual marks in the field throughout the years.

Positioned on the south side of the road, the benchmark RN11 on the upper slope, was also missing, along with all of the other bench and fixed marks in the area (Fig. 2).

In the first set of data (Fig. 5) there appear to be more benchmarks which haven't been surveyed in the past campaigns due to their damages. Most of the remaining benchmarks show small variations, however there are two benchmarks, RN4 and RN7 which appear to have the highest variation by comparison with all the other benchmarks, and these are found inside the area marked as active landslide which is already known.

In the eastern part of the survey area, the data along the road towards the opposite side compared to the position of the dam, all of the benchmarks seem to still be in the right place, bench marks RN 13-31 (Fig. 2). At least from this point of view, this area appears to be more stable. In this set (Fig. 6) it appears that the benchmarks with the highest displacement are represented by the group of RN17-19 and RN26, which are placed near the road adjacent to the area marked as displaced area of debris in figure 2. The characteristic of the site in set 2 (Fig. 6) is overall one described by subsidence with only one bench mark placed in an area with uplift, RN31 (Figs. 2 and 6). Comparing 2017 with 2012 data it appears that the overall trend is of an increasing negative displacement in the majority of the benchmarks, with a few exceptions at the RN26-30 benchmarks with the situation almost reversed.

These data shows the complexity of the site in terms of the active landslide, with the area closer to the dam clearly more affected by the landslide compared to the area furthest away from the dam, which appears to be significantly more stable. On the top of the road, closer to the RN7 benchmark,

the orthomosaic resulting from the airborne surveys with the drone, visibly highlights a distinctive area in the road where the pavement is significantly damaged (Fig. 7), appearing darker in the data. The orthophotomosaic provides a cm level precision image which allows for a better in depth analysis of the damages created by the active landslide in the area. The darker patch on the side of the road closer to the lake, also shows a slight subsidence as well on top of the significant visible damage, however character changes while following the road more to the east, where the road appears significantly in a better shape. The orthophotomosaic allows for visualising several features like cracks in the pavement for example (Fig. 8), where this crack for example appears to have a spread of approximately 0.15 cm and an elevation change of approximately 4 mm. Information like this is very useful if repetitive surveys are carried out regularly for measuring how much these cracks develop in time and to calculate at what rate these are developing.

The other set of data resulted from the airborne surveys with the drone, is represented by the DEM's, which allows for a better overview of the different elevation differences in the area and better highlight deformations at the surface which won't be visible to the naked eye. Elevation profiles (Fig. 9) in different areas of the DEM, highlight the difference in elevation throughout the whole data set and surveyed area. This way it is possible to see with a really high precision, the change in elevation across the profile (Fig. 9e-f). In the shorter profiles across the width of the road (Fig. 9b-d) different deformations and variations can be seen of about 10-15 cm running across the profiles, showing irregularities throughout the whole length of the profiles.





**Fig. 7.** An overview of the orthophotomosaic created from the airborne surveys.

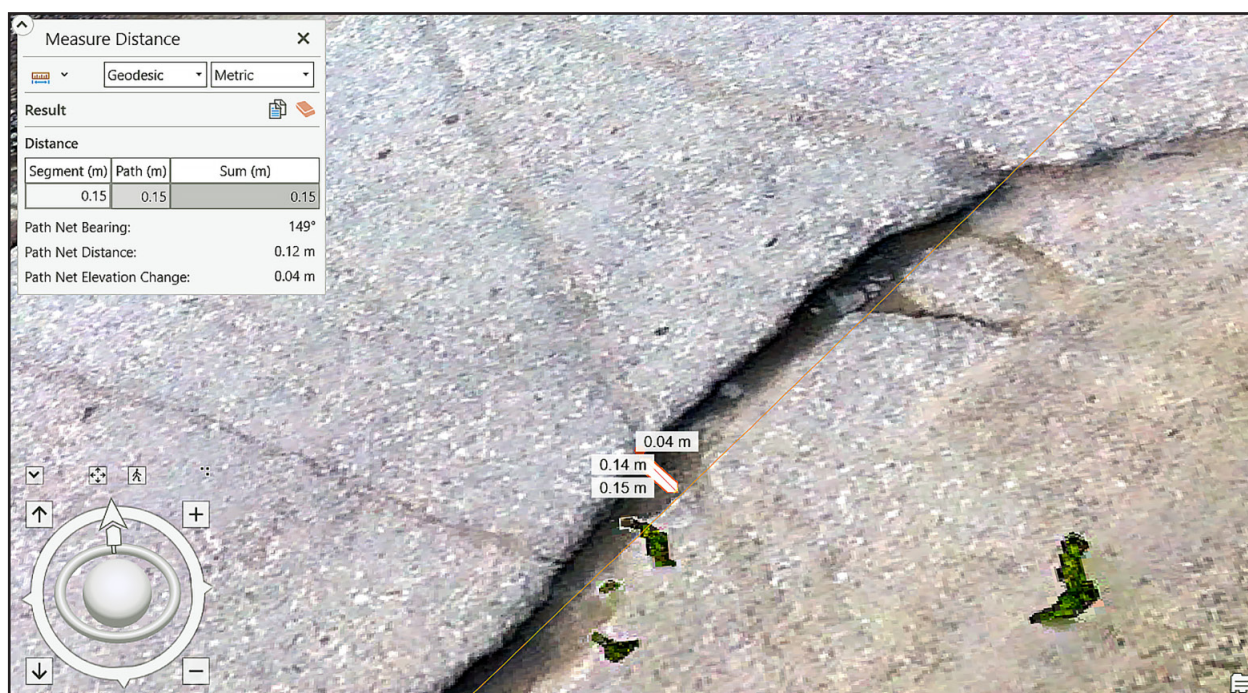


**Fig. 8.** The high resolution of the orthophotomosaic data allows for measuring dimensions of the cracks in the road.

All of the profiles and data show slight subsidences appearing in the area closer to the landslide marked in the levelling network figure (Fig. 2), and subsidence in the range of 10 cm in the area which appears darker and visibly appearing with damaged concrete at the surface visible in the orthophotomosaic (Fig. 7).

Apart from these data, the orthophotomosaic and the DEM, resulted from the airborne surveys with the drone, the survey proved to be very efficient in highlighting the areas

marked with spray at the end of the GPR profiles (Fig. 10). Therefore allowing for a better positioning of the GPR profiles in GIS and allowing for comparing and following areas of interest across all of the methods.

In terms of GPR data, all of the profiles have been processed and analysed. The data appears to show some different characteristics across all of the profiles, which indicate the complexity of the site, however there are also similarities throughout the profiles (Fig. 11).

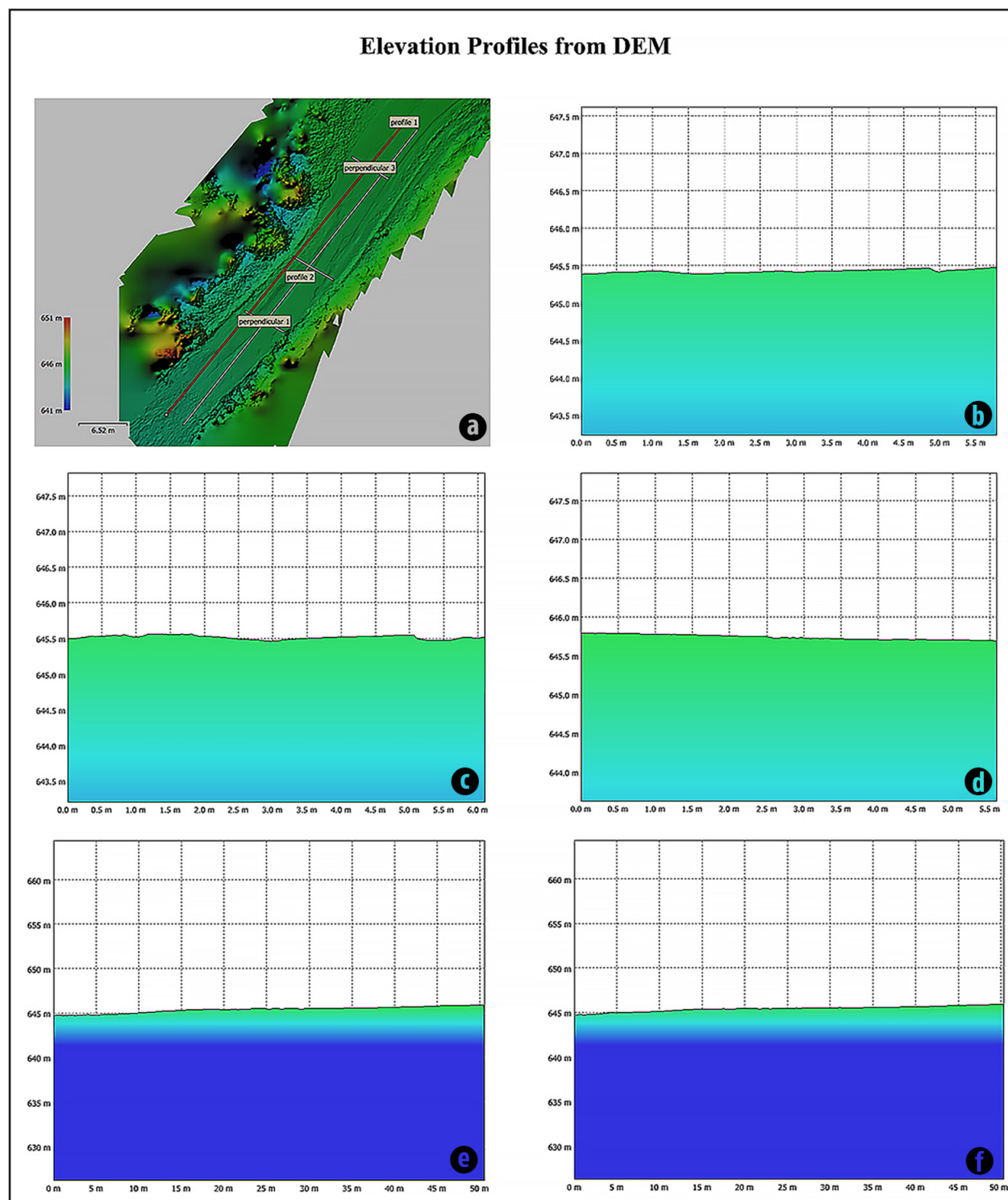


**Fig. 9.** The DTM resulted from the airborne surveys and elevation profiles from different sections with the focus on the deterioration area: (a) overview of the DEM and the elevation profile location; (b) perpendicular profile 1; (c) perpendicular profile 2; (d) perpendicular profile 3; (e) longitudinal profile 1; (f) longitudinal profile 2.





**Fig. 10.** The quality of the orthophotomosaic allows for detecting the end of the GPR profiles marked with spray on the pavement.

In the profiles closer to the upper side of the slope (Fig. 11a-b) the horizon appearing (marked with red) at approximately 30 ns, appears to appear sooner at about 20 ns in the profiles closer to the edge of the slope on the side with the lake (Fig. 11c-d). Comparing the data with site notes but also when overlapping with the orthophotomosaic, this is a clear consequence of the almost complete absence of the concrete layer from the surface of the road in the area mostly affected by the deformations. This horizon (marked with the red line) is different from the area underneath through to the fact that from 0 ns to 20-30 ns, there appear to be multiple reflection in the form of hyperbolas, which might indicate an area with a higher degree of rubble or ballast normally used at these types of roads.

Other features appear as well in the data as it is the anomaly appearing in figure 11a, marked as a possible geological feature, due to the strong large sized reflective area. As this does not appear on any other profiles it has been marked as of natural source, due to the fact that it has no lateral continuity. Other feature of interest highlighted in figure 11b, is represented by the stronger reflective horizon area, which might indicate an area of possible pockets of air, as the electromagnetic waves travel faster in air and the horizon still seems rather continues, so the shape itself does not change but the character or permittivity. In the last two profiles, which are closer to the down slope (towards the lake), noting that the profile in figure 11d is longer than profile in figure 11c, as it was acquired to cover the section really close to the margin of the road, there appears a feature which is marked by a stronger reflection but with a complex shape. This has been interpreted as a deformation with a

subsidence character due to its lowering shape, and the change in reflectivity marking the change in permittivity. It is interesting however that it appears on two parallel profiles, which means that the features are slightly larger than 0.5 m. The last feature is only apparent in the last profile (Fig. 11d), here the character of the anomaly appearing as a stronger reflection in an area which generally appears homogeneous, and with the multitude of overlapping hyperbolas which might indicate the path of the electromagnetic waves bouncing from different sides inside the void.

A general remark about the GPR data is that there are no significant features in the form of reflections appearing below 40-50 ns or about 1.5 m when calculated with the 0.06 m/ns velocity. This is interesting in itself due to the fact that the 200 MHz antenna was used with the purpose of collecting information from deeper layers, and the fact that this was not possible might indicate the character of the environment which is predominantly represented by clays. The visible wet areas in the area, observed when collecting the data, might indicate that the clays are also wet which absorbs the signal even more, not allowing for the signal to allow for reflections from deeper areas.

#### 4. CONCLUSIONS

This study successfully demonstrates the integration of Ground Penetrating Radar (GPR), airborne photogrammetry, and traditional levelling data as a robust and efficient approach for rapid terrain analysis in landslide-prone areas, especially near important infrastructure like the Poiana Ruscă dam in Romania.



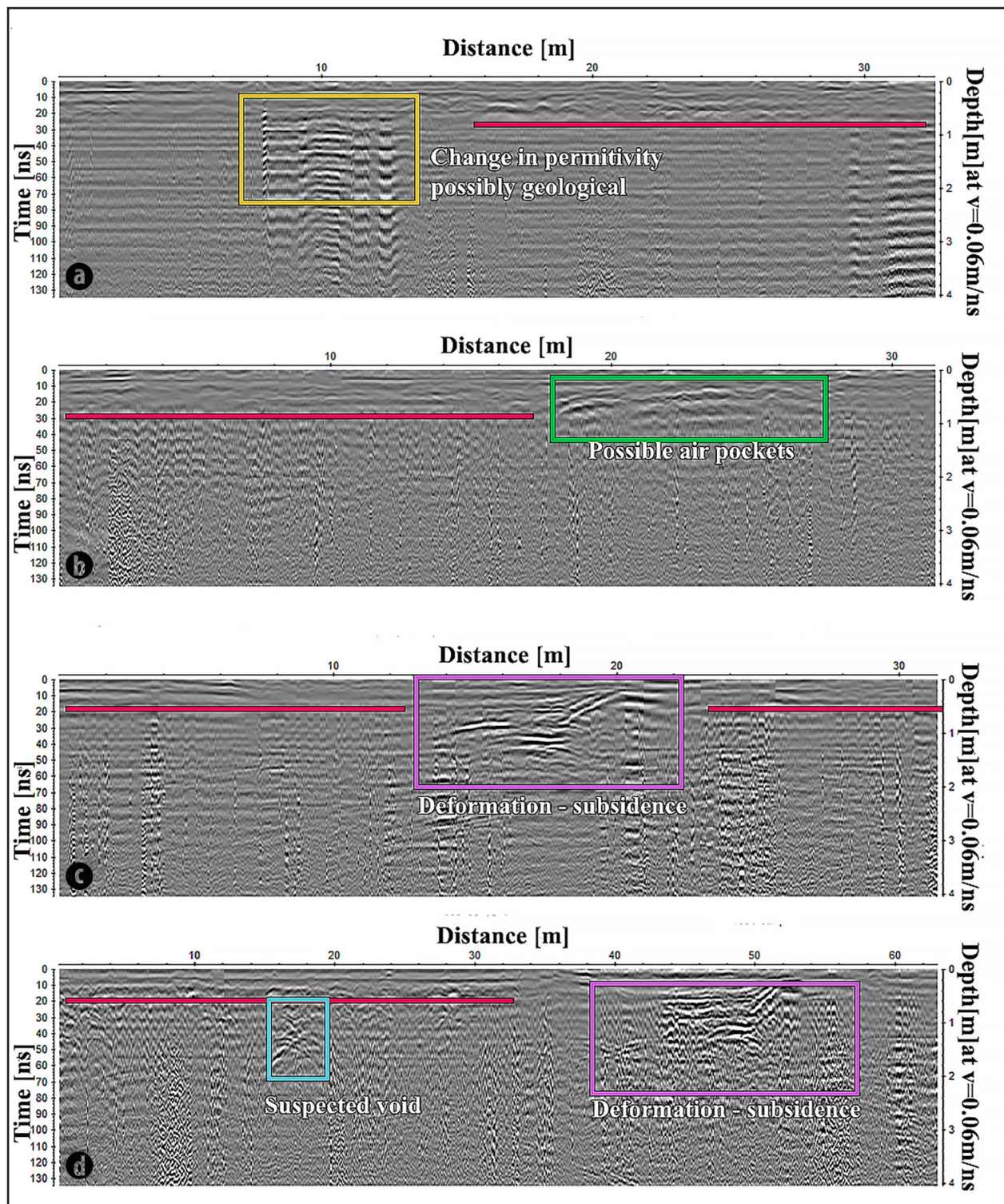


**Fig. 11.** The processed GPR profiles: (a) furthest away from the edge of the slope; (b) profile in the middle of the road; (c) profile on the edge of the slope; (d) longer profile at the maximum possible edge of the slope.

The synergy between these technologies enhances the understanding of landslide dynamics, offering both surface and subsurface perspectives.

The utilisation of compact drones for orthophotomosaics and Digital Elevation Models (DEMs) has proven to be a valuable tool in assessing surface deformations with high-resolution data. Concurrently, GPR, particularly with a 200 MHz antenna, has shown its efficacy in revealing some subsurface features which are not accessible through traditional levelling method, like the imaging of the potential subsidence areas, voids, and alterations in subsurface composition and moisture content, which are vital for understanding the landslide's structure and dynamics.

Some challenges faced in traditional levelling methods, such as the loss of benchmarks due to terrain movements are addressed, and the integration of GPR and photogrammetry helps in overcoming these limitations by providing additional data that aids in forming a more comprehensive understanding of the landslide's behaviour.

The findings of this study are particularly significant for the maintenance and safety of the Poiana Ruscă dam and its surrounding infrastructure. They also set a precedent for the application of these methods in the continuous monitoring and management of other geohazards, especially in the context of maintaining the integrity of hydropower dams and related infrastructure. The identification of small-scale subsidence and voids, as well as the detection of changes in the subsurface environment, contribute to the early detection and mitigation of potential risks associated with landslides. As it is the case with the levelling annual or biannual surveys, the GPR and photogrammetry surveys should also be carried out regularly, in order to provide a more comprehensive characterization and understanding of the behaviour of the landslide and its development in time. With more repetitive data in time, in different seasons and different conditions, especially for the GPR data, more information can be retrieved from the area.

The study signifies a step forward in the field of geohazard monitoring. It showcases how modern technology can be harnessed to enhance the safety and stability of crucial infrastructure, emphasising the importance of ongoing innovation and adaptation in topo-geodetical and geophysical investigation methods. It also provides practical aspects which can help with future decision making about the repairing of the roads for example, in the area. As it is normally the case, the roads affected by the landslide, are normally repaved, more ballast and stone is added in an area which has problems with the subsidence, and especially as the GPR highlights some more acute (even though small in dimensions) deformations and subsidence zones under the surveyed road. Adding more materials on top will probably only put more pressure and accelerate the subsidence, therefore more measures need to be taken and more GPR surveys combined with airborne surveys, to assess where consolidation measures need to be taken in advance of any repairs.

In conclusion, this research not only contributes significantly to the field of landslide monitoring but also serves as a model for the effective application of advanced technologies in environmental management and infrastructure safety.

## ACKNOWLEDGEMENTS

The authors wish to express their deep gratitude to Prof. Dr. Eng. Cornel Păunescu and Cornel & Cornel Topoexim SRL for their invaluable contribution and support during this project. They also extend their thanks to Roxana Stănescu for their assistance in the topo-geodetical aspects of the research. Appreciation is also extended to Gere Gheorghe for his crucial support and logistical assistance in collecting geophysical data. Special thanks are due to Dr. Eng. Traian Moldoveanu, Mihai Duțu, and Mihaela Istrate for supplying geophysical equipment.

## REFERENCES

- 
- ALTAWHEEL, M., KHELIFI, A., LI, Z., SQUITIERI, A., BASMAJI, T., GHAZAL, M. (2022). Learning on Optical UAV Imagery: Preliminary Results. *Remote Sensing*, **14**: 553.
- BATRAKOV, D.O., ANTUFUEYEVA, M.S., ANTUFUEYEV, A.V., BATRAKOVA, A.G. (2017). GPR data processing for evaluation of the subsurface cracks in road pavements. 9th International Workshop on Advanced Ground Penetrating Radar (IWAGPR): 1-6, Edinburgh, UK.
- BIANCHINI CIAMPOLI, L., TOSTI, F., ECONOMOU, N., BENEDETTO, F. (2019). Signal Processing of GPR Data for Road Surveys. *Geosciences*, **9**: 96.
- BORECKA, A., HERZIG, J., DURJASZ-RYBACKA, M. (2015). Ground Penetrating Radar Investigations of Landslides: A Case Study in a Landslide in Radziszów. *Studia Geotechnica et Mechanica*, **37**.
- BUSETTI, A., CALLIGARIS, C., FORTE, E., AREGGI, G., MOCNIK, A., ZINI, L. (2020). Non-Invasive Methodological Approach to Detect and Characterize High-Risk Sinkholes in Urban Cover Evaporite Karst: Integrated Reflection Seismics, PS-InSAR, Leveling, 3D-GPR and Ancillary Data. A NE Italian Case Study. *Remote Sens.*, **12**: 3814.
- CONYERS, L.B. (2004). Ground-Penetrating Radar for Archaeology. Alta Mira Press, Walnut Creek, 203 p.

- COȘARCĂ, C. (2003). Topografie inginerească, Ed. Matrix Rom, București.
- DANIELS, D.J. (2004). Ground Penetrating Radar. 2nd Edition, IEE Radar, Sonar and Navigation Series, **15** (Ed.). The Institution of Electrical Engineers, London.
- DE GIORGI, L., LEUCCI, G. (2014). Detection of Hazardous Cavities Below a Road Using Combined Geophysical Methods. *Surv Geophys.*, **35**: 1003-1021.
- KNYAZ, V.A., CHIBUNICHEV, A.G. (2016). Photogrammetric Techniques for Road Surface Analysis. *ISPRS - International Archives of the Photogrammetry, Remote Sensing and Spatial Information Sciences*, **XLI(B5)**: 515-520.
- MUGNAI, F., LONGINOTTI, P., VEZZOSI, F., TUCCI, G. (2022). Performing low-altitude photogrammetric surveys, a comparative analysis of user-grade unmanned aircraft systems. *Applied Geomatics*, 0123456789.
- PĂUNESCU, C., SPIROIU, I., PĂUNESCU, V. (2010). Curs de geodezie-topografie. Editura Universității din București.
- RASOL, M., PAIS, J.C., PÉREZ-GRACIA, V., SOLLA, M., FERNANDES, F.M., FONTUL, S., AYALA-CABRERA, D., SCHMIDT, F., ASSADOLLAHI, H. (2022). GPR monitoring for road transport infrastructure: A systematic review and machine learning insights. *Construction and Building Materials*, **324**: 126686.
- REYNOLDS, J.M. (2011). An Introduction to Applied and Environmental Geophysics, New York, NY: Wiley-Blackwell.
- RHAZI, J., DOUS, O., KAVEH, S. (2004). Detection of Fractures in Concrete by the GPR Technique. 16th World Conference on NDT, Montreal, Canada.
- SESTRAS, P., BILAȘCO, Ș., ROȘCA, S., VERES, I., ILIES, N., HYSĂ, A., SPALEVIĆ, V., CÎMPEANU, S.M. (2022). Multi-Instrumental Approach to Slope Failure Monitoring in a Landslide Susceptible Newly Built-Up Area: Topo-Geodetic Survey, UAV 3D Modelling and Ground-Penetrating Radar. *Remote Sens.*, **14**: 5822.
- STANKOVIĆ, M., MIRZA, M.M., KARABIYIK, U. (2021). UAV forensics: DJI mini 2 case study. *Drones*, **5**(2): 1-20.
- SUN, J., YUAN, G., SONG, L., ZHANG, H. (2024). Unmanned Aerial Vehicles (UAVs) in Landslide Investigation and Monitoring: A Review. *Drones*, **8**: 30.
- ULLAH, F., SU, L.J., ALAM, M. ET AL. (2022). Landslide stability investigation and subsurface deformation mapping by optimizing low-frequency GPR: A mega rainfall susceptible landslide case study (Gilgit Baltistan, Pakistan). *Bull Eng Geol Environ.*, **81**: 373.